Reliability of numerical wind tunnels for VAWT simulation

2016 J. Phys.: Conf. Ser. 753 082025

(http://iopscience.iop.org/1742-6596/753/8/082025)

Reliability of numerical wind tunnels for VAWT simulation

M. Raciti Castelli[1], M. Masi[1], L. Battisti[2], E. Benini[2], A. Brighenti[2], V. Dossena[3], G. Persico[3]

[1] Department of Management and Engineering
University of Padova, Stradella S. Nicola 3 - 36100 Vicenza, I
[2] Department of Civil, Environmental and Mechanical Engineering
University of Trento, via Mesiano 77 - 38123 Trento, I
[3] Energy Department
Politecnico di Milano, via Lambruschini 4 - 20158 Milano, I

E-mail: marco.raciticastelli@unipd.it

Abstract. Computational Fluid Dynamics (CFD) based on the Unsteady Reynolds Averaged Navier Stokes (URANS) equations have long been widely used to study vertical axis wind turbines (VAWTs). Following a comprehensive experimental survey on the wakes downwind of a troposkien-shaped rotor, a campaign of bi-dimensional simulations is presented here, with the aim of assessing its reliability in reproducing the main features of the flow, also identifying areas needing additional research.

Starting from both a well consolidated turbulence model (k-ω SST) and an unstructured grid typology, the main simulation settings are here manipulated in a convenient form to tackle rotating grids reproducing a VAWT operating in an open jet wind tunnel. The dependence of the numerical predictions from the selected grid spacing is investigated, thus establishing the less refined grid size that is still capable of capturing some relevant flow features such as integral quantities (rotor torque) and local ones (wake velocities).

1. Introduction

The concept of vertical axis wind turbine (VAWT) design has been pursued by researchers with some demonstrable success during the last decades. As a matter of fact, even though a widespread use of such technology is still far from being achieved, VAWTs exhibit a certain number of advantages over their horizontal counterparts, especially in turbulent wind conditions that generally characterize the urban environment. Consequently, literature reviews regarding VAWTs [1] and [2] state that an in-depth knowledge of their distinctive flow physics could be of the utmost importance for future developments.

Despite their geometrical features being relatively simple (especially the H-rotor blades, which appear as a trivial extrusion of a bidimensional airfoil section), VAWT architectures experience inherently unsteady aerodynamics due to the continuous variation of the blade angle of attack and Reynolds number during their revolution, resulting in a highly distorted and time dependent wake evolution downstream of the rotor, as evidenced by [3] and [4] by resorting to the particle image velocimetry (PIV). Such phenomena, typical of slow rotating machines, produce a significant effect on both the dynamic loadings acting on the rotor and the generated power,

ultimately affecting the turbine overall performance. Moreover, the resulting wake meandering downstream of the rotor (for detailed investigation of the evolution of the wake downstream of a VAWT, see [5] [6]) is impossible to investigate through classical aerodynamic tools, such as the Blade Element - Momentum (BE-M) method and calls for the use of Computational Fluid Dynamics (CFD), which can better model complex flow structures. As a matter of fact, CFD based on the Unsteady Reynolds Averaged Navier Stokes (URANS) equations have long been widely used to study wind energy conversion systems. Being VAWTs dominated by flow unsteadiness, such approach can be considered the ideal trade-off between accuracy, where Large Eddy Simulations (LES) should conceptually better reproduce flow separation from the blades and rotor wake, and computational cost, where Blade Element - Momenutm (BE-M) methods assure very fast response.

On the other hand, it is well known that the accuracy of a CFD calculation strongly relies on physical and numerical modelling (see e.g., turbulence closure and temporal or spatial schemes, respectively) as well as the type and the level of refinement choosen for the computational grid (see e.g., structured vs unstructured meshes and cell size, respectively). Moreover, the extension of the computational domain plays its role as well. Finally, it is well known that CFD simulations are computationally demanding if compared with BE-M and their actual reliability is often an open issue, particularly if prior validation is not available (for some information about general guidelines to be used in CFD, see [7]). This is due to a general lack of knowledge on experimental information and physical phenomena occurring during rotor operation, thus limiting the validation process to a mere comparison between measured and predicted power performance. In light of this, the definition of a generally accepted roadmap for verification and validation of VAWT simulations is necessary. Thus, the ultimate objective of the here presented work is two-fold: on the one hand, to assess the reliability of simulations aimed at predicting VAWT operation by using CFD URANS approaches; on the other, to identify areas needing additional research and development.

Even though open field tests should ideally represent the optimal benchmark for numerical simulations (due, e.g., to the absence of blockage effects), they prompt several problems in terms of stability and control of the incoming flow conditions. On the other hand, wind tunnel tests allow to collect data in controlled flow conditions and avoid the inevitable disturbance due to the surrounding environment. Following a previous work ([8]) in which the theoretical requirements for a time accurate unsteady CFD simulation of VAWTs operation have been assessed, the present work investigates the counterpart needings of such type of simulations to allow for results of integral values (such as torque and power) and local ones (velocities) that do not depend on the grid refinement. Because a full three-dimensional simulation is quite demanding in terms of CPU resources and time, and in order to perform the most accurate numerical validation of the CFD model with a reasonable computational cost, the presented study focuses on the 2D simulation of the VAWT symmetry plane, where tri-dimensional effects (e.g., axial/spanwise gradients and velocity components) are absent. However, following an experimental research program carried out in the frame of an European granted project ("DeepWind", launched in autumn 2010 under "FP7 Future Emerging Technologies" [9]), part of the results obtained in a wind tunnel experimental campaign on a troposkien rotor are used here to attempt also an experimental validation of the numerical simulations. Thus, local values of the flow field within the rotor wake were measured in the horizontal plane placed at rotor midspan, and compared with the predictions derived from a moving grid transient simulation of the rotor operating at optimal tip speed ratio, trying to assess the reliability of the CFD predictions obtained by means of the implemented numerical settings.

Using the commercial simulation code Ansys Fluent and a well consolidated simulation setup (e.g., the combination of k-ω SST turbulence model and a second order implicit scheme to compute unsteady flows on unstructured meshes), generally accepted in wind turbine CFD [10]

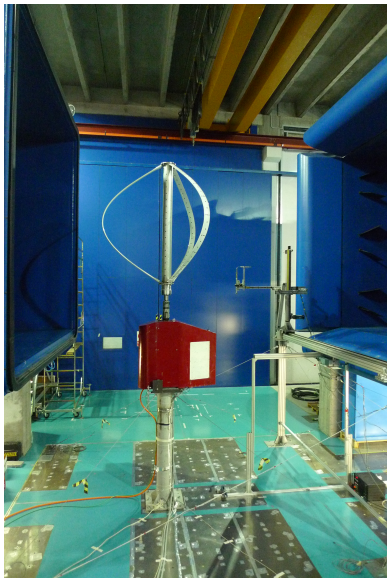

Figure 1. Side view of the test arrangement.

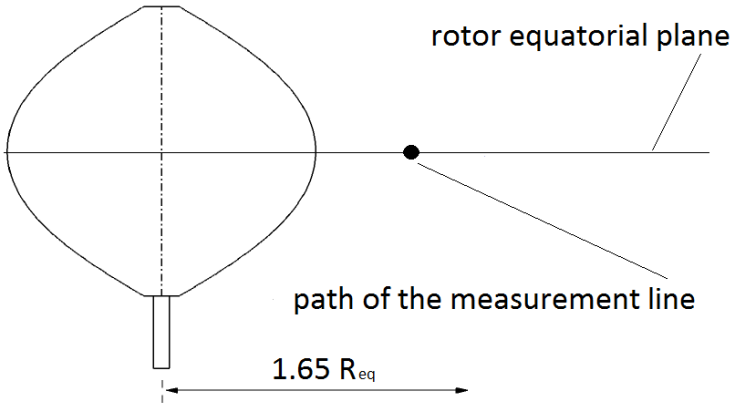

Figure 2. Quoted scheme of the wake measurement line downstream of the rotor.

[11] [12], the effect of grid density around the blade profiles and within the inner region of the computational domain that encloses the rotor are investigated. The proposed numerical study can therefore be intended as a contribution to the formalization of general guidelines for the simulation of VAWTs. Even though further work should be necessary to extend the results obtained here, this research would hopefully help the on-going debate about the definition of a consolidated and generally accepted numerical approach to be used in the simulation of wind turbines.

2. Experimental methodology

The hereby proposed numerical simulations were supported by experiments performed in the large scale wind tunnel of the Politecnico di Milano (IT), using the high speed section (4.00 m wide $\cdot$ 3.84 m high) in a free-jet configuration (achieved by removing the test section and operating the rotor in a jet boundary confined environment). High flow quality was obtained by resorting to honeycombs and anti-turbulence screens, leading to a freestream turbulence intensity lower than 1% at test section.

The DeepWind reduced scale demonstrator is a troposkien rotor of equatorial radius $R_{eq} = 1.014$ m. It is characterized by a height/diameter ratio $\beta = H/(2R_{eq}) = 0.97$ and is composed by three glass fibre blades laid up over a central foam core. A constant blade section of chord $c = 0.101$ m, extending from hub to hub (for more details, see [13] [14] [15] [16]), is characterized by a DU-06-W200 asymmetric airfoil, derived from the more common NACA 0018 profile and specifically modified for VAWT applications with some promising results, such as [17]:

- an increase in structural strength without a corresponding decrease in performance;
- a higher maximum lift coefficient for positive angles of attack;
- improved self-starting properties and higher power outputs at low tip speed ratios due to a slight camber;
- a shift of the deep stall condition towards higher angles of attack, combined with a smaller drop in the lift coefficient;
- the absence of a laminar separation bubble, which entails a significant noise reduction.

Figure 1 provides a view of the test arrangement, showing both the open jet chamber and the instrumented rotor, which was centered with respect to the incoming free-jet. To assess the validity of the proposed experiments and their exploitation for numerical code validation, a preliminary quantification of the resulting blockage was conducted using established correlations available in literature, based on the work of [18] and applied in the formulation adapted and proposed by [19]. The resulting global blockage correction coefficient was close to 3% (see [20]) and was therefore considered negligible for the scope of the present work.

The measurement apparatus, briefly recalled in the present section, is extensively reported in [19]. Rotor angular velocity was provided by an absolute encoder, while the aerodynamic torque transmitted through the shaft was measured by resorting to a precision torquemeter mounted between elastic joints. An 8-poles synchronous motor/generator with a rated power of 8.6 kW was installed on the power train and controlled using an inverter, thus assuring a constant rotational speed during the whole measurement campaign.

As shown in Figure 2, wake measurements were conducted in an horizontal line, normal to the incoming wind and located 1.5 radii downstream of the rotor test section, by means of a motorized traversing system mounting a directional five hole probe and two hot wire probes for measuring the pressure and velocity fields. Uncertainty in the velocity measurement resulted about 2% after calibration on a low-speed jet (for further information about the measurement apparatus, see also [21]).

3. Numerical methodology

The present simulations aim at investigating the bi-dimensional flow field at the equatorial plane of the rotor. A bi-dimensional computational domain is therefore discretized by two grids: a (fixed) outer one, where also the main geometrical features of the wind tunnel are modelled (Figure 3), and a (rotating) inner one, containing the three blade arrangements and the rotor shaft, revolving at the very same angular velocity of the turbine (Figure 4).

Turbulence kinetic energy and V_∞ at the domain inlet are fixed to 1 m^2/s^2 and to 6.7 m/s, respectively (in accordance to the available experimental data), whereas the zero gradient condition is imposed at the domain outlet. *Wall* boundary conditions are imposed at the tunnel walls, while *symmetry* (i.e. normal derivatives of dependent variables equal to zero) boundary conditions are given to the external boundaries of the entire computational domain,

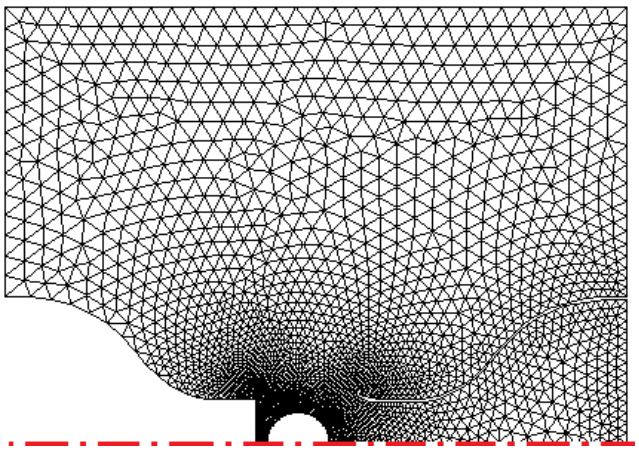

Figure 3. External computational domain; being depicted with respect to the longitudinal wind tunnel axis, only half of the domain is represented.

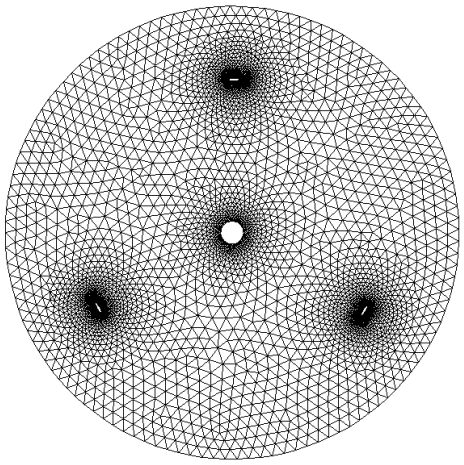

Figure 4. Internal (rotating) computational domain, not in scale.

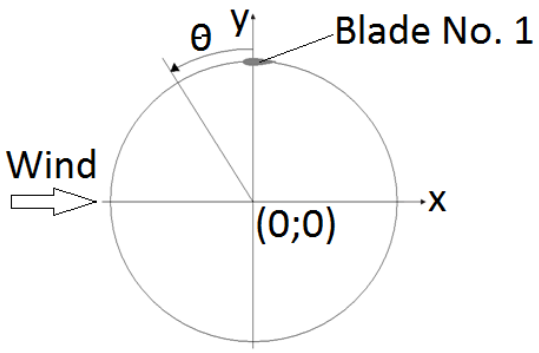

Figure 5. Adopted reference system for rotor blade position.

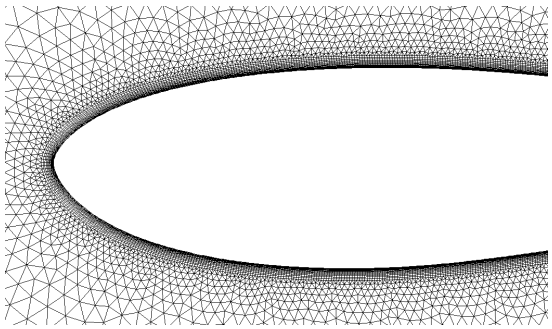

Figure 6. Near blade mesh showing the structured boundary layer.

corresponding to the physical walls of the building where the wind tunnel is located.

Rotor azimuthal position is identified by the angular coordinate of blade No. 1 quarter-chord, starting at the axis dividing the first and the second Cartesian plane quadrants, as shown in Figure 5.

Triangular meshes are adopted for both the inner and the outer domains. Each blade is located inside a control circle of four chords diameter, required to better control the dimension of the grid elements in the near blade zone. A structured near wall layer is developed along each blade. Figure 6 shows some details of the mesh surrounding the rotor blade, while Table 1 summarizes its main features. After completing such structured layer, the near blade mesh is built by adopting an appropriate size function, operating from the blade profile to the control circle. A second size function, operating from the (three) control circles to the remaining rotating region, ends with grid elements featuring the same size of the facing cells in the outer fixed grid. The sensitivity to both grid spacing along each blade profile, and at the boundary of the rotating grid, on wake characteristics and rotor torque is investigated by resorting to six meshes, respectively characterized by 40, 80, 160, 320, 480 and 640 grid points along each half-blade profile. The value selected for the height of the first cell layer allows obtaining a mean y^+ value (computed over each blade) close to 1 for every azimuthal coordinate. Moreover, the effect of grid spacing inside the rotating domain is investigated by resorting to a maximum grid dimension at the outer boundary of the moving grid of 40, 80 and 160 mm.

Table 1. Main features of the near blade mesh.

Description	Value
Height of the first cell layer [mm]	0.03
Growth factor from blade surface [-]	1.15
Number of structured layers along each blade [-]	14
Maximum grid spacing at the outer boundary of the moving grid [mm]	40, 80, 160

The Reynolds Averaged Navier-Stokes (RANS) equations are solved using a finite-volume method with a segregated solution strategy. The governing equations are discretized by a second order upwind scheme.

The well known $k-\omega$ SST turbulence model is here adopted, due to its capability of describing flow separation [22] [23] which occurs in flow fields dominated by adverse pressure gradients, even if it shows a certain sensitivity to grid size [24].

The simulated operating condition is that of the rotor revolving at an angular speed of 220 rpm (i.e. $\Omega = 23.04$ rad/s), that corresponds to a tip speed ratio at the equatorial plane equal to:

$$\lambda_{eq} = \frac{\Omega R_{eq}}{V_\infty} = 3.49 \tag{1}$$

Each simulation is run until the instantaneous values of the torque coefficient are less than 1% compared to the corresponding values of the previous period of 120° rotor revolution, due to its three-bladed architecture, in formula:

$$C_T(\theta) = \frac{T(\theta)}{0.5\rho A R_{eq} {V_\infty}^2} \tag{2}$$

being $T(\theta)$ the aerodynamic torque on the rotor (2D) section, ρ the air mass density (set at the constant value of 1.225 kg/m^3, A the swept area of the simulated 2D section (equal to the product of $2R_{eq}$ and the conventional height of a bidimensional simulation (i.e. 1 m). The residuals for each physical time step and governing equation are set to 10^{-5}.

An angular marching step of 0.25° is selected according to the findings in [8]. The present simulations are performed by a 2.33 GHz quad-core processor with Hyper-Threading; the CPU time for simulations involving between 60.000 and 200.000 grid elements is about 24-48 hours.

4. Results and discussion

The measured torque coefficient at $\lambda_{eq} = 3.49$ is equal to 0.09. It corresponds to a torque per unit area swept by the rotor equal to 2.6 N/m, whereas the corresponding CFD value is 3.8 N/m. Note that the last datum is the only integral value that could be used to roughly compare experiments with results of 2D simulations at rotor mid-span, even though the experimental value derives from a rotor characterized by a continuously changing radius (from the maximum value, at the equator, to virtually zero at both upper and bottom sections). As a matter of fact, a direct comparison between measured and computed torque and thrust is not applicable because all the performance measurements account for the entire (three-dimensional) rotor arrangement. However, a sort of experimental validation is discussed in the subsection that follows the next one.

4.1. Numerical validation of the model

Figure 7 shows the influence of the selected grid spacing (along each half-blade profile) on the predicted rotor torque coefficient. The values are normalized with respect to the asymptotic torque resulted from the computation performed on the most refined grid (i.e., the grid featuring 640 cells along each blade pressure/suction side). It clearly appears that the grid size strongly affects the prediction of the rotor performance; it is definitively recognized that the requested cell number for obtaining satisfactory results is quite high (i.e. on the order of 400-500 grid points along each half-blade profile, that correspond to about 100.000 cells required to simulate the only midspan plane under the still ideal 2D flow assumption!). Such a high value is necessary to correctly simulate the flow separation due to adverse pressure gradients occurring on rotor blades during their revolution, especially in those azimuthal positions where high relative angles of attack (clearly belonging to the post-stall region) determine a complex interaction between

vortices released from the blades leading and trailing edges. This statement is supported by Figure 8, that shows the evolution of the pressure coefficient, defined as:

$$c_p = \frac{p - p_\infty}{0.5\rho(\Omega R_{eq})^2} \tag{3}$$

along the curvilinear coordinate of blade No. 1 suction side for $\theta = 90°$ (i.e. directly facing the incoming freestream). The curvilinear coordinate is normalized, starting from blade leading edge ($s/t = 0$) up to blade trailing edge ($s/t = 1$). A marked underestimation of the computed pressure can be noticed for the most coarse grids (i.e. 40 and 80 grid cells along the half-blade profile), while an asymptotic behaviour is clearly visible in the case of the finest grid refinements. Note that the local profile of the static pressures show vanishing differences between the finest grid refinements (i.e. 160 and 320, further refinements are not here pictured for clarity's sake, being the resulting graphs almost overlapping), whereas global values (i.e. the torque coefficient, Figure 7) still differ, even though almost close to the asymptotic range. This means that there are other local flow features captured by the simulation that did not yet reach their asymptotic values when the prediction of the flow field around the blades has already become not dependent on the grid size. It can be concluded that both integral and local properties should be considered to evaluate the minimum grid size required to calculate VAWT global performance that does not change whether an even more refined grid is considered.

On the other hand, Figure 9 shows that the computed rotor performance appears to be less affected by the grid spacing inside the rotating domain (at least for the tested cell dimensions): as a matter of fact, while quadrupling the cell size along the blade profile with respect to the lowest tested dimension (that assures the grid independence) determines a reduction of the simulated torque higher than 16% (see again Figure 7), the same operation at the interface between the fixed grid and the rotating one affects the simulated torque less than 2% (see Figure 9).

Even though the above described requirements do not appear as a problem for bidimensional simulations, they became a severe constraint when tackling with three-dimensional modelling, resulting the necessary cell number (in the order of tens of millions) potentially out of the reach of most of the adopted simulation computers.

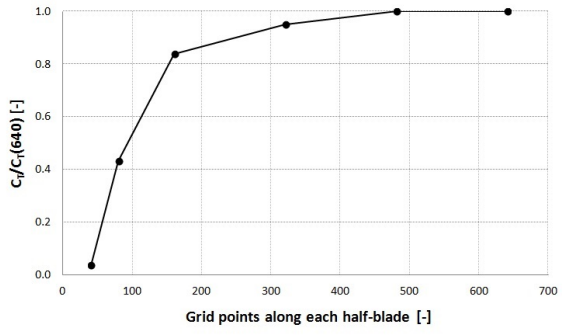

Figure 7. Influence of grid points number along each blade pressure/suction surface on the computed torque coefficient, normalized with respect to the value obtained using the finer grid spacing (i.e. 640 points along each blade pressure/suction side).

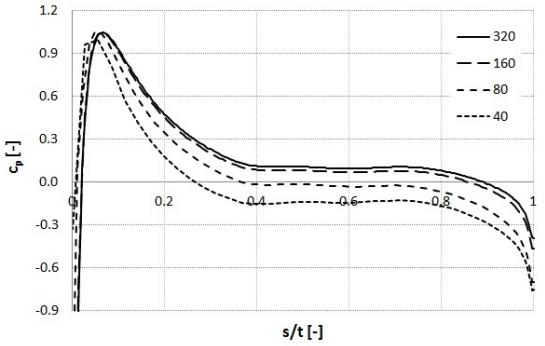

Figure 8. Influence of grid points number along each blade on the evolution of the pressure coefficient along blade No. 1 suction side ($\theta = 90°$).

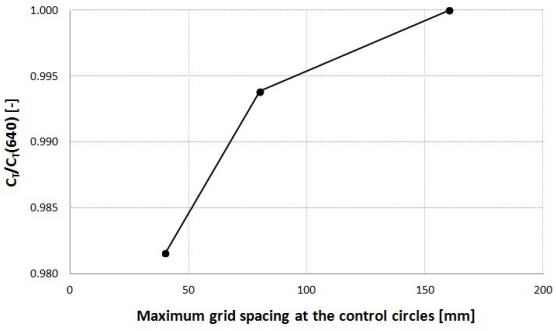

Figure 9. Effect of the maximum grid spacing at the outer boundary of the rotating region (i.e. at the interface between the fixed grid and the rotating one) on the computed torque coefficient.

Figure 10 shows a comparison between measured longitudinal velocity data (V_x) and computed ones along the horizontal line (at right angle with respect to the incoming freestream) located 1.65 radii downstream of the rotor axis, as shown in Figure 2. Again, a marked influence of the selected grid refinement along each blade is apparent and the requirement of about 400-500 grid points along the blade profile, previously stated, for a pressure distribution along the blade no more dependent on the grid size, is confirmed by the wake analysis as well. Thus, it is concluded that these two-dimensional calculations need almost 65.000 quadrangular/triangular cells in the moving region and a total of about 100.000 cells in the entire domain. Accordingly, almost 80-100 million of cells is an optimistic estimation for the minimum cells number required to perform fully three-dimensional unsteady calculations of VAWTs that predict global performance parameters and local flow field values that do not change by refining the grid when thetrahedral mesh embedding prismatic near-wall layers are used.

This conclusion of the numerical validation complements the findings of a previous study ([8]) about the time step size required by unsteady calculations of VAWT operation and confirms the mandatory requirement of the experimental validation of any URANS-CFD analysis, especially when the latter do not benefit of computational resources that still today are not available for most of the analysts.

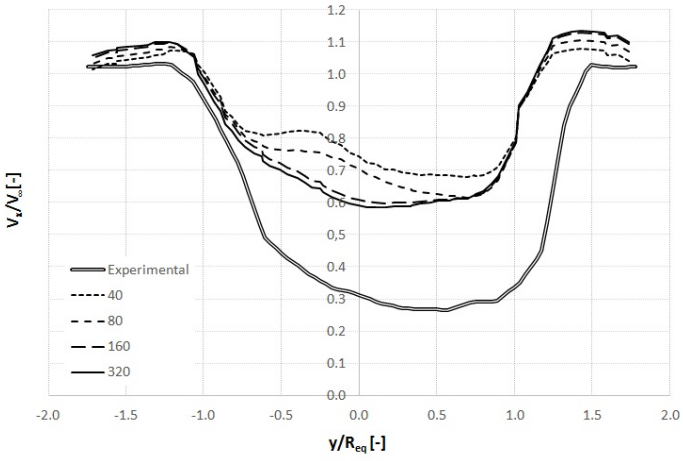

Figure 10. Comparison between the longitudinal velocity (i.e. along the x axis), normalized with respect to the incoming freestream velocity ($V_\infty = 6.7$ m/s), predicted by the CFD model and the one measured 1.65 rotor equatorial radii downstream of the test section.

4.2. Experimental validation of the model

Although the global trend of the relevant features in the wake axial velocity is acceptably predicted, the comparison with the experimental values clearly shows the apparent effect of the computational domain blockage. In fact, the two-dimensional domain that encloses the VAWT

equatorial section constrains within the rotor symmetry plane the entire flow diffusion due to the power extraction performed by the turbine, whereas the actual flow spreads also outward from the symmetry plane, especially when a troposkien architecture is considered. In fact, the CFD simulation:

- predicts an unrealistic increase of the longitudinal velocity up to 8 m/s aside the central portion of the computational domain (it is here recalled that the wake roughly resembles the swept area of the simulated rotor section, see [20]);
- determines a contraction of the wake downstream of the rotor, being the flow forced to re-enter the wind tunnel aft the open test section, as qualitatively shown by the streamline plot in Figure 11;
- limits the typical (see [3] and [19]) horizontal asymmetry of the wake, determining a shift in the peak of the momentum loss of about 1/4 R_{eq}. In fact, the increased blockage in the positive y range (i.e. where the blades travel against the incoming flow) forces a relatively high wake velocity, instead of the marked velocity deficit apparent in the experimental velocity profile (due to the more effective work extraction in the second Cartesian plane quadrant); on the contrary, the lower blockage in the negative y range (i.e. where the blades travel in the same direction of the incoming flow) allows for a better agreement between computed and measured velocity values.

In summary, the main effect of the flow field on the performance at rotor midspan, due to the flow blockage originated by this two-dimensional CFD calculation, is two-fold:

- a small over-estimation of the wind velocity at the upwind part of the VAWT (i.e., a predicted local value of λ slightly lower than the actual one);
- a relevant over-estimation of the wind velocity at the downwind part of the VAWT (i.e., a local λ notably lower than the actual one).

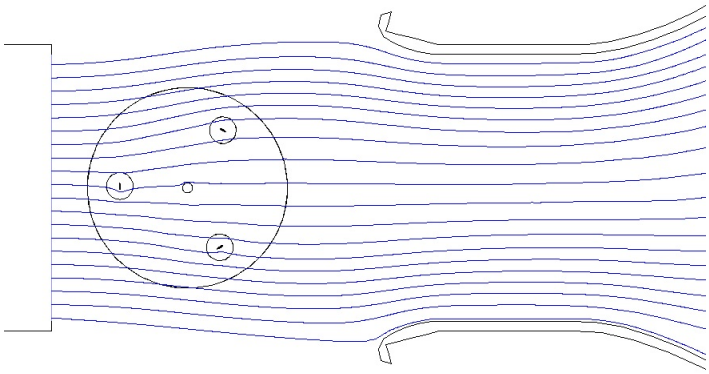

Figure 11. Wake contraction downstream of the rotor, visualized by means of absolute pathlines.

All the presented findings strongly compromise the reliability of two-dimensional calculations and, accordingly, rise many doubts on the at-first-sight higher reliability of VAWT performance prediction based on two-dimensional CFD, if compared with other seeming less-accurate approaches (see, e.g., BE-M method). However, in order to gain some insight on the reliability expected also from three-dimensional CFD calculations, two additional computations are here proposed on the grid counting 320 cells along the half-blade profile. Inlet and outlet boundary conditions are changed for both computations (from velocity inlet to fixed pressure and from pressure outflow to fixed velocity, respectively), in order to better simulate the suction operated by the arrays of fans located downstream of the wind tunnel diffuser in the experimental facility. In addition, one of the two simulations features also a reduction in the flow rate (thus trying

to account for the previously discussed blockage effect); this latter is roughly estimated as follows: the spatially averaged axial velocity at the measurement section can be calculated by integration of the area underlying the experimental data in Figure 10, while an uniform velocity equal to the VAWT upstream value is tentatively assumed in the remaining part of the wind tunnel width. According to this very simplified structure assumed for the actual flow field, a gross estimate of an average axial velocity equal to 5.2 m/s (i.e., about 77% of the upstream velocity) is obtained. Thus, the light-blue dot line in Figure 12 reports the time averaged axial velocity at the measurement line, predicted as if the entire upstream flow remains on the midspan plane, whereas the light-blue point line reports the scenario in which the 23% of the plane flow approaching the VAWT diffuses in the vertical direction without passing through the measurement line. Comparing these lines with the experimental data (black line in Figure 12), it is worth noting that:

- although the amplitude of the flow blockage effect is not modified, the change in boundary conditions determines a better agreement between CFD results and experiments, in terms of qualitative trend and features of the wake (see the more symmetrical velocity distribution in the outer region of the wake and both the ripples and the slope of the CFD velocity defect, that appears to copy the experiments if the shift toward negative abscissae of about $1/4R_{eq}$ - previously discussed - is considered);
- the modification of the mean velocity magnitude within the domain necessarily (by continuity constraint) increases the agreement between calculated and measured time averaged velocity values. However, the overall extension of the wake and the wake shift towards negative y coordinates are almost unaffected by such velocity reduction, even though the trend of the curve is (very sightly) improved.

Figure 12 also shows the time averaged velocity profiles calculated by CFD along the lines located at $1.15R_{eq}$ and $2R_{eq}$ (see the red and the green lines, respectively) downstream of the VAWT test section. Accordingly, the time averaged spatial evolution of the wake downstream of the rotor, as predicted by both the actual and the reduced upstream velocity calculations, shows that the higher the downstream location:

- the higher the reduction of the velocity defect in both the magnitude and the y-wise amplitude;
- the higher the recovery of the wake symmetry and the approaching of the minimum axial velocity location to the x axis origin.

The previous findings drive to conclude that the absence of the spanwise diffusion:

- confirms the increased effect of the aft wind tunnel walls. This occurrence alters the time averaged velocity profiles outside from the velocity defect zone, by increasing/decreasing the value of the maximum/minimum velocity and, accordingly, rising the hump in the numerical profile that is not measured by the experiments;
- forces the computed wake to develop in advance and also to close within a region spatially less extended than what occurs in the actual experiment case.

On the other hand, comparing the predictions of wake evolution at a different upstream velocity, it clearly appears that, although the reduction of the upstream velocity increases the extension of the region occupied by the wake development and smooths the gradients in the velocity profiles that become (slightly) more similar to the experimental data, important differences that can not be ascribed to the limits of the two-dimensional approach still remain. This last issue prompts for additional work, required to state the accuracy expected also by three-dimensional computations. In fact, it is not yet quantified the effect on the accuracy of VAWT performance prediction due to:

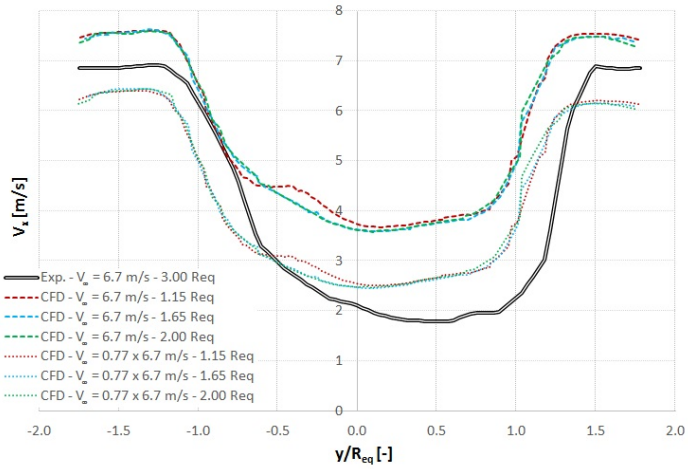

Figure 12. Comparison between the longitudinal velocity (i.e. along the x axis) predicted by the CFD model, at different positions downstream of the rotor test section and also for a 77% reduced unperturbed freestream, and the one measured 1.65 rotor equatorial radii downstream of the test section.

- the well-known artificial dissipation (say, numerical diffusivity) related with triangular grids (i.e., thetrahedral cells in the three-dimensional case). This is expected to be limited by using either structured grids (i.e., hexahedral cells in the three-dimensional case) or polyhedral grids [25], being the latter less diffusive than thetrahedal grids and more suited to fit complex geometrical domains without requiring the useless refinements of some spatial regions that is unavoidable when structured grids are considered.
- the capability of the selected turbulence model to deal with turbulent anysotropy effects, as compared to either different two-equations Non Linear Eddy Viscosity Models (NVLM), usually available in commercial codes, or to other two-equations NVLM that already demonstrated to perform well when anysotropy effects are important, without the need of additional computational cost [26].

5. Conclusions

When treating the operation of VAWTs in controlled conditions, numerical simulations must be carefully calibrated in terms of spatial discretization. This choice has to take into account not only the minimization of the huge CPU time required by an unsteady moving mesh simulation, but also the fulfilment of several numerical restrictions.

Using a well consolidated turbulence model, the effect of a poor choice in discretizing the near blade zone appears to be very significant in terms of both local and integral properties, while a reduced effect is registered by a coarse refinement in the outer region of the rotating grid. The here presented simulations, performed on unstructured triangular grids with near wall quadrilateral cells layers, reached predictions of global performance that do not depend on grid size only by resorting to a very high cell number (for a bi-dimensional computation), consisting in nearly 500 grid points deployed on each blade pressure/suction surface, thus requiring almost 65.000 quadrangular/triangular cells in the moving region and a total of about 100.000 cells in the entire domain. It can be certainly concluded that the present achievements prompt a dramatic increase of CPU times required to have numerically validated results, especially as far as three-dimensional simulations are concerned.

Despite the massive computational effort required to perform three-dimensional computations on grids size estimated to be in the order of 100 million cells, it is likely that the computed velocities in the wake still appear to miss the measured data (even though the general shape of the wake is correctly reproduced) according to the results of the two-dimensional simulations performed here. However, the evaluation of the accuracy expected by a three-dimensional CFD model of a VAWT is far to be concluded. In view of the practical infeasibility of studies on

the grid spacing performed directly on the actual three-dimensional domain, two-dimensional CFD computations appear to be still required, in spite of the fact (that it is shown here) that the two-dimensional hypothesis of the flow field does not hold, also at the midspan plane of troposkien VAWTs. Accordingly, further work is recommended, with the aim of extending the here presented preliminary findings to a more general result. In particular, it seems to be necessary:

(i) experimental works that make available to the analysts i) more data on the spatial evolution of the wake at rotor downstream; ii) data on VAWTs geometry better suited to two-dimensional models (see, e.g., the H-shaped Darrieus VAWT, that is expected to show a lower spanwise diffusion at midspan);

(ii) numerical simulations aimed at quantifying i) the effective reduction of numerical diffusion when triangular grids are substituted by either the difficult-to-build structured grids or the promising polyhedral cells; ii) the increase in the accuracy of the prediction when other two-equations non linear eddy viscosity models, that are able to better capture turbulence anisotropies without increase the computational effort, are adopted.

List of symbols

Latin

A	rotor swept area [m^2]
c	rotor blade chord [m]
C_T	torque coefficient [-]
D_{eq}	rotor equatorial diameter
H	rotor height [m]
p	static pressure [Pa]
R_{eq}	rotor equatorial radius [m]
s	curvilinear coordinate along the pressure or suction side of rotor blade [m]
R_{eq}	rotor equatorial radius
t	length of the pressure or suction side of rotor blade [m]
T	aerodynamic torque [Nm]
V_x	wind speed along the longitudinal axis [m/s]
V_∞	freestream wind speed [m/s]
x	longitudinal coordinate (i.e. along the freestream direction) [m]
y	transversal coordinate (i.e. normal to the freestream direction) [m]

Greek

β	ratio between rotor height and diameter [-]
Θ	azimuthal blade position [°]
λ_{eq}	tip speed ratio computed at the equatorial section [-]
ρ	air density [kg/m^3]
Ω	rotor angular velocity [rad/s]

Acronyms

BE-M	Blade Element-Momentum
CFD	Computational Fluid Dynamics
LES	Large Eddy Simulation
NVLM	Non Linear Eddy Viscosity Models
RANS	Reynolds Averaged Navier Stokes
SST	Shear Stress Transport

URANS Unsteady Reynolds Averaged Navier Stokes
VAWT Vertical Axis Wind Turbine

Acknowledgements
The authors would like to thank Uwe S. Paulsen and the other members of the DeepWind project team for providing the VAWT demonstrator and for funding the wind tunnel campaign. The DeepWind project was supported by the European Commission (FP7/2007-2013), Grant Agreement No. 256769 on "Energy 2010 - Future emerging technologies".

References

[1] H. J. Sutherland, E. Berg Dale, T. D. Ashwill, "A Retrospective of VAWT Technology", SAND2012-0304.
[2] M. M. A. Bhutta, N. Hayat, A. U. Farooq, Z. Ali, S. R. Jamil, Z. Hussain, "Vertical Axisd Wind Turbine - A Review of Various Configurations and Design Techniques", Renewable and Sustainable Energy Reviews, Vol. 16(4), pp. 1926-1939.
[3] C. J. S. Ferreira, G. J. W, van Bussel, G. A. M. van Kuik, "Wind Tunnel Hotwire Measurements, Flow Visualization and Thrust Measurement of a VAWT in Skew", Journal of Solar Engineering, Vol. 128(2006), pp. 487-497.
[4] C. J. S. Ferreira, G. J. W, van Bussel, F. Scarano, "2D PIV Visualization of Dynamic Stall on a Vertical Axis Wind Turbine", 45^{th} AIAA Aerospace Sciences Meeting, Reno, Nevada (US), Jan. 8-11, 2007.
[5] F. Trivellato, M. Raciti Castelli, "Appraisal of Strouhal number in wind turbine engineering", Renewable and Sustainable Energy Review, Vol. 49 (2015), pp. 795-804.
[6] G. Persico, V. Dossena, B. Paradiso, L. Battisti, A. Brighenti, E. Benini, "Three-Dimensional Character of VAWT Wakes: an Experimental Investigation for H-Shaped and Troposkien Architectures", 2016, ASME paper GT2016-57762, Proceedings of the ASME Turbo Expo 2016: Turbomachinery Technical Conference and Exposition, June 13-17, 2016, Seoul, (KR).
[7] AIAA-G-077-1998, "Guide for the Verification and Validation of Computational Fluid Dynamics Simulations", American Institute of Aeronautics and Astronautics, 1998.
[8] F. Trivellato, M. Raciti Castelli, "On the Courant-Friedrichs-Lewy criterion of rotating grids in 2D vertical-axis wind turbine analysis", Renewable Energy, Vol. 62 (2014), pp. 53-62.
[9] U. S. Paulsen, H. A. Madsen, K. A. Kragh, P. H. Nielse, I. Baran, J. H. Hattel, E. Ritchie, K. Leban, H. Svendsen, P.A. Berthelsen, "DeepWind-from idea to 5 MW concept", Energy Procedia, Vol. 53 (2014), pp. 23-33.
[10] M. H. Mohamed, A. M. Ali, A. A. Hafiz, "CFD analysis for H-rotor Darrieus turbine as a low speed wind energy converter", Engineering Science and Technology, an International Journal, Vol. 18 (2015), pp. 1-13.
[11] L. A. Danao, J. Edwards, O. Eboibi, R. Howell, "The Performance of a Vertical Axis Wind Turbine in Fluctuating Wind - A Numerical Study", WCE 2013, July 3 - 5, 2013, London (UK).
[12] K. Suffer, R. Usubamatov, G. Quadir, K. Ismail, "Modeling and Numerical Simulation of a Vertical Axis Wind Turbine Having Cavity Vanes", 2014 Fifth International Conference on Intelligent Systems , Modelling and Simulation, January 27 - 29, 2014, Langkawi (MY).
[13] T. F. Pedersen, U. S. Paulsen, L. Vita, H. A. Madsen, P. H. Nielsen, K. A. Kragh, K. Enevoldsen, S. A. Sørensen, M. Rasmussen, R. Kjaersgaard, C. B. Pedersen, K. Clemmensen, L. Battisti, L. Zanne, A. Brighenti, J. Wedell-Heinen, V. Lim, J. Yi Ho, I. Lee, E. Ritchi, M. Leban Krisztina, G. van Bussel, G. Tescione, S. Carstensen, P. A. Berthelsen, C. Smadja, "Design and Manufacture of an Offshore Concept Wind Turbine - the DeepWind Demonstrator, Tech. Rep. E-0030, DTU Wind Energy, May 2013.
[14] U. S. Paulsen, L. Vita, H. A. Madsen, J. H. Hattel, E. Ritchie, K. Leban, P. A. Berthelsen, S. Carstensen, "1st DeepWind 5 MW baseline design", Energy Procedia, Vol. 24(2012), pp. 27-35.
[15] U. S. Paulsen, H. A. Madsen, J. H. Hattel, I. Baran, P. H. Nielsen, "Design Optimization of a 5 MW Floating Offshore Vertical-Axis Wind Turbine", Energy Procedia, Vol. 35 (2013), pp. 22-32.
[16] L. Vita, "Offshore Floating Vertical Axis Wind Turbines with Rotating Platform", PhD Thesis, Technical University of Denmark, Aug. 2011.
[17] U. S. Paulsen, T. F. Pedersen, H. A. Madsen, K. Enevoldsen, P. H. Nielsen, J. Hattel, L. Zanne, L. Battisti, A. Brighenti, M. Lacazeand, V. Lim, J. W. Heinen, P. A. Berthelsen, S. Carstensen, E. J. de Ridder, G. van Bussel, G. Tescione, W. He, "DeepWind - An Innovative Wind Turbine Concept for Offshore", EWEA 2011 Conference, Brussels (BE), Mar. 14-17, 2011.
[18] E. Mercker, J. Wiedemann, "On the correction of interference effects in open jet wind tunnel", Tech. Rep. 960671, SAE International, 1996.

[19] V. Dossena, G. Persico, B. Paradiso, L. Battisti, S. Dell'Anna, E. Benini, A. Brighenti, "An experimental study of the aerodynamics and performance of a vertical axis wind turbine in confined and unconfined environment", Journal of Energy Resources Technology, Vol. 137, Iss. 5.
[20] L. Battisti, E. Benini, A. Brighenti, M. Raciti Castelli, V. Dossena, G. Persico, U. S. Paulsen, T. F. Pedersen, "Wind Tunnel Testing of the DeepWind Demonstrator in Design and Tilted Operating Conditions", Energy, Vol. 111 (2016), pp. 484-497.
[21] V. Dossena, G. Persico, B. Paradiso, L. Battisti, S. Dell'Anna, E. Benini, A. Brighenti, "An Experimental Study of the Aerodynamics and Performance of a Vertical Axis Wind Turbine in Confined and Unconfined Environment", ASME Journal of Energy Resources Technology, Vol. 137 (2015), 051207-1-12.
[22] P. R. Spalart, "A One-Equation Turbulence Model for Aerodynamic Flows", Recherche Aerospatiale, No. 1 (1994), pp. 5-21.
[23] F. R. Menter, "Two-Equation Eddy-Viscosity Turbulence Models for Engineering Applications", AIAA Journal, Vol. 32, Iss. 8, pp. 1598-1605.
[24] J. E. Bardina, P. G. Huang, T. J. Coakley, "Turbulence Modeling Validtion, Testing and Development", NASA Technical Report 110446, 1997.
[25] M. Peric, "Flow Simulation using Control Volumes of Arbitrary Polyhedral Shape", Ercoftac Bulletin, No. 62, 2004.
[26] M. Antonello, M. Masi, "A Simplified Explicit Algebraic Model for the Reynolds Stresses", Int. J. Heat Fluid Flow, Vol. 28, Iss. 5 (2007), pp. 1092-1097.